

Residual Networks of Residual Networks: Multilevel Residual Networks

Ke Zhang, *Member, IEEE*, Miao Sun, *Student Member, IEEE*, Tony X. Han, *Member, IEEE*, Xingfang Yuan, *Student Member, IEEE*, Liru Guo, and Tao Liu

Abstract—Residual networks family with hundreds or even thousands of layers dominate major image recognition tasks, but building a network by simply stacking residual blocks inevitably limits its optimization ability. This paper proposes a novel residual-network architecture, Residual networks of Residual networks (RoR), to dig the optimization ability of residual networks. RoR substitutes optimizing residual mapping of residual mapping for optimizing original residual mapping, in particular, adding level-wise shortcut connections upon original residual networks, to promote the learning capability of residual networks. More importantly, RoR can be applied to various kinds of residual networks (Pre-ResNets and WRN) and significantly boost their performance. Our experiments demonstrate the effectiveness and versatility of RoR, where it achieves the best performance in all residual-network-like structures. Our RoR-3-WRN58-4 models achieve new state-of-the-art results on CIFAR-10, CIFAR-100 and SVHN, with test errors 3.77%, 19.73% and 1.59% respectively. These results outperform 1001-layer Pre-ResNets by 18.4% on CIFAR-10 and 13.1% on CIFAR-100.

Index Terms—Image classification, Residual networks, Residual networks of Residual networks, Shortcut, Stochastic Depth.

I. INTRODUCTION

CONVOLUTIONAL Neural Networks (CNNs) have given the computer vision community a significant shock [1], and have been improving state-of-the-art results in many computer vision applications. Since AlexNets' [2] groundbreaking victory at the ImageNet Large Scale Visual Recognition Challenge 2012 (ILSVRC 2012) [4], deeper and deeper CNNs [2], [3], [5], [6], [7], [8], [9], [10], [11], [12] have been

This work is supported by National Natural Science Foundation of China (Grants No. 61302163 and No. 61302105), Hebei Province Natural Science Foundation (Grants No. F2015502062) and the Fundamental Research Funds for the Central Universities.

K. Zhang is with the Department of Electronic and Communication Engineering, North China Electric Power University, Baoding, Hebei, 071000 China e-mail: zhangkeit@ncepu.edu.cn.

M. Sun is with the Department of Electrical and Computer Engineering, University of Missouri, Columbia, MO, 65211 USA e-mail: msqz6@mail.missouri.edu.

T. X. Han is with the Department of Electrical and Computer Engineering, University of Missouri, Columbia, MO, 65211 USA e-mail: HanTX@missouri.edu.

X. Yuan is with the Department of Electrical and Computer Engineering, University of Missouri, Columbia, MO, 65211 USA e-mail: xyuan@mail.missouri.edu.

L. Guo is with the Department of Electronic and Communication Engineering, North China Electric Power University, Baoding, Hebei, 071000 China e-mail: glr9292@126.com.

T. Liu is with the Department of Electronic and Communication Engineering, North China Electric Power University, Baoding, Hebei, 071000 China e-mail: taoliu@ncepu.edu.cn.

Manuscript received , 2016; revised , 2016.

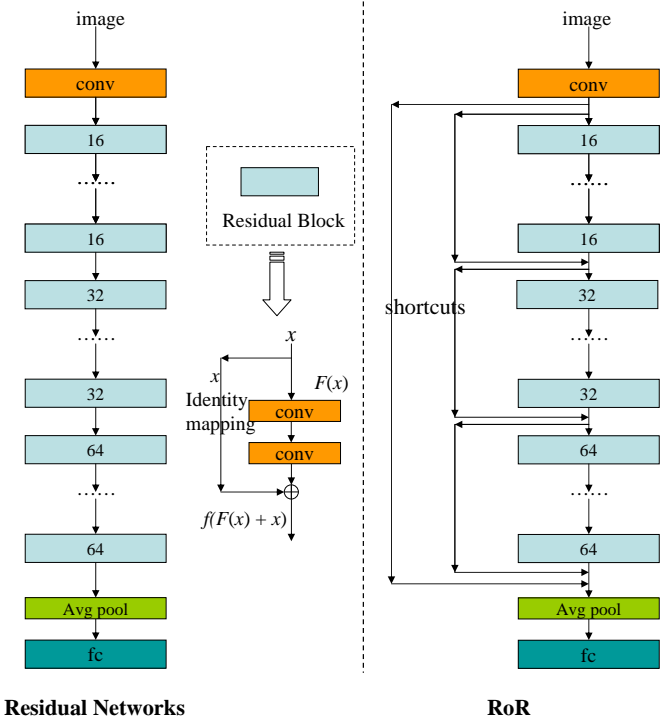


Fig. 1. The left image with dashed line is an original residual network which contains a series of residual blocks, and each residual block has one shortcut connection. The number (16, 32, or 64) of each residual block is the number of output feature map. $F(x)$ is the residual mapping and x is the identity mapping. The original mapping represents as $F(x) + x$. The right image with dashed line is our new residual networks of residual networks architecture with three levels. RoR is constructed by adding identity shortcuts level by level based on original residual networks.

proposed and achieved better performance on ImageNet or other benchmark datasets. The results of these models revealed the importance of network depth, as deeper networks lead to superior results.

With a dramatic increase in depth, residual networks (ResNets) [12] achieved the state-of-the-art performance at ILSVRC 2015 classification, localization, detection, and COCO detection, segmentation tasks. However, very deep models will suffer vanishing gradients and over-fitting problems, thus the performance of thousand-layer ResNets is worse than hundred-layer ResNets. Then the Identity Mapping ResNets (Pre-ResNets) [13] simplified the residual networks training by BN-ReLU-conv order. Pre-ResNets can alleviate vanishing gradients problem, so that the performance of thousand-layer Pre-ResNets can be further improved. The

latest Wide Residual Networks (WRN) [14] treated vanishing gradients problem by decreasing depth and increasing width of residual networks. Nevertheless, the exponentially increasing number of parameters brought by broader networks worsens the over-fitting problem. As a result, dropout and drop-path methods are usually used to alleviate over-fitting, and the leading method on ResNets is Stochastic Depth residual networks (SD) [15] which can improve the test accuracy and reduce training time in the meantime. No matter what kind of residual networks they are, they all based on one basic hypothesis: By using shortcuts connections, residual networks perform residual mapping fitted by stacked nonlinear layers, which is easier to be optimized than the original mapping [12]. Furthermore, we hypothesize that the residual mapping of residual mapping be easier to be optimized than original residual mapping. So based on this hypothesis, we can construct a better residual-network architecture to enhance performance.

In this paper, we present a novel and simple architecture called Residual networks of Residual networks (RoR). Firstly, comparing with the original one-level-shortcut-connection ResNets, we add extra shortcut connections on original ResNets level by level. A multilevel network is then constructed, as seen in Fig. 1. For this network, we analyze the effects of different shortcut level numbers, shortcut types and maximum epoch numbers. Secondly, in order to alleviate over-fitting, we train RoR with drop-path method, and obtain apparent performance boost. Thirdly, we build RoR on various residual networks (Pre-ResNets and WRN), and we find out that RoR is suitable to not only original ResNets but also other residual networks. Through massive experiments on CIFAR-10, CIFAR-100 [16] and SVHN [17], our RoR can dig as much optimization ability of the residual networks as possible, only by adding a few shortcuts. Although this approach seems quite simple, it is surprisingly effective in practice, and achieves the new state-of-the-art results on above datasets.

Our main contribution is threefold:

We introduce RoR which improve the optimization ability of ResNets. RoR can easily be constructed by adding a few identity shortcuts on ResNets, and achieve better performance than ResNets with the same number of layers.

We elucidate that our RoR is also suitable to other residual networks and boost their performance. Our RoR is an important and effective complement of residual networks family.

Through experiments, we analyse the effects of different depth, width, shortcut level numbers, shortcut types and maximum epoch numbers to RoR, and give reasonable strategies to construct RoR.

The remainder of the paper is organized as follows. Section II briefly reviews related works for deep convolutional neural networks and residual networks family. The proposed RoR method is illustrated in Section III. The optimization of RoR is described in Section IV. Experimental results and analysis are presented in Section V, leading to conclusions in Section VI.

II. RELATED WORK

A. Deeper and Deeper Convolutional Neural Networks

In the past several years, deeper and deeper CNNs have been constructed, because the more convolutional layers are in CNNs, the better optimization ability CNNs can obtain. From 5-conv+3-fc AlexNet (ILSVRC2012 winner) [2] to the 16-conv+3-fc VGG networks [7] and 21-conv+1-fc GoogleNet (ILSVRC2015 winner) [11], both the accuracy and the depth of CNNs were increasing. But very deep CNNs face a crucial problem, vanishing gradients [18]. Earlier works adopted initialization methods and layer-wise training to reduce this problem [19], [20]. Moreover, ReLU activation function [21] and its variants ELU [22], PReLU [23], PELU [24] also can prevent vanishing gradients. Fortunately, this problem can be largely addressed by batch normalization (BN) [25] and carefully normalized weights initialization [23], [26] according to recent research. BN [25] standardized the mean and variance of hidden layers for each mini-batch, while MSR [23] initialized the weights by more reasonable variance. In another aspect, a degradation problem has been exposed [27], [28], [12] that is, not all systems are similarly easy to optimize. In order to resolve this problem, several methods were proposed. Highway Networks [28] consisted of a mechanism allowing 2D-CNNs to interact with a simple memory mechanism. Even with hundreds of layers, highway networks can be trained directly through simple gradient descent. ResNets [12] simplified Highway Networks using a simple skip connection mechanism to propagate information to deeper layers of networks. ResNets are more simple and effective than highway Networks. Recently, FractalNet [29] generated an extremely deep network whose structural layout was precisely a truncated fractal by repeating application of a single expansion rule, and this method showed that residual learning was not required for ultra-deep networks. However, in order to get the competitive performance as ResNets, FractalNet need much more parameters than ResNets. Now more and more residual network variants and architectures [13], [30], [31], [24], [14], [32], [15], [33], [34] have been proposed, and they form a residual networks family together.

B. Residual Networks Family

The basic idea of ResNets [12] is that residual mapping is easy to optimize, so ResNets skip blocks of convolutional layers by using shortcut connections to form shortcut blocks (residual blocks). These stacked residual blocks greatly improve training efficiency and largely resolve the degradation problem by employing BN [25] and MSR [23]. The ResNets architecture and residual block are shown in Fig. 1, where each residual block can be expressed in a general form:

$$\begin{aligned} y_l &= h(x_l) + F(x_l, W_l), \\ x_{l+1} &= f(y_l) \end{aligned} \quad (1)$$

Where x_l and x_{l+1} are input and output of the l -th block, F is a residual mapping function, $h(x_l) = x_l$ is an identity mapping function and f is a ReLU function. However, the vanishing gradients problem still exists, as the test result of 1202-layer ResNets is worse than 110-layer ResNets on CIFAR-10 [12].

In the Pre-ResNets, He et al. [13] created a direct path for propagating information through the entire network by both $h(x_l)$ and f being identity mappings. The residual block of Pre-ResNets performs the follow computations:

$$x_{l+1} = h(x_l) + F(x_l, W_l) \quad (2)$$

The new residual block with BN-ReLU-conv order can reduce training difficulties, so that Pre-ResNets can get better performance than original ResNets. More importantly, Pre-ResNets can reduce vanishing gradients problem even for 1001-layer Pre-ResNets. Inspired by Pre-ResNets, Shen et al. [33] proposed weighted residuals for very deep networks (WResNet), which removed the ReLU from highway and used weighted residual functions to create a direct path. This method can also train 1000+ layers residual networks, and achieve good accuracy. In order to further reduce vanishing gradients, Shah et al. [31] and Trottier et al. [24] proposed the use of ELU and PELU respectively instead of ReLU in residual networks.

Besides vanishing gradients problem, over-fitting is another challenging issue for CNNs. Huang and Sun et al. [15] proposed a drop-path method, Stochastic Depth residual networks (SD) which randomly dropped a subset of layers and bypassed them with the identity mapping for every mini-batch. SD can alleviate over-fitting and reduce vanishing problem, so it is a good complement of residual networks. By combining dropout and SD, Singh et al. [32] proposed a new stochastic training method, SwapOut, which can be viewed as an ensemble of ResNets, dropout ResNets and SD ResNets.

Recently, more variants of residual networks are proposed, and they all promote learning capability by expending width of model. Resnet in Resnet (RiR) [30] was a generalized residual architecture which combines ResNets and standard CNNs in parallel residual and non-residual streams. WRN [14] decreased depth and increased width of residual networks by adding more feature planes, and achieves the latest state-of-the-art results on CIFAR-10 and SVHN. The newest Convolutional Residual Memory Networks (CRMN) [34] were inspired by WRN and Highway Networks. CRMN augment convolutional residual networks with a long short term memory mechanism based on WRN, and achieve the latest state-of-the-art performance on CIFAR-100. These wider residual networks indicate that wide and shallow residual networks result in good performance and can easy training.

III. RESIDUAL NETWORKS OF RESIDUAL NETWORKS

RoR is based on a hypothesis: To dig the optimization ability of residual networks, we can optimize the residual mapping of residual mapping. So we add shortcuts level by level to construct RoR based on residual networks.

Fig. 2 shows the original residual network with L residual blocks. These L original residual blocks are denoted as the final level of shortcuts. Firstly, we add a shortcut above all residual blocks, and this shortcut can be called root shortcut or first level shortcut. Generally we use 16, 32 and 64 filters sequentially in the convolutional layers [12], [13], and each kind of filter has $L/3$ residual blocks which form three residual

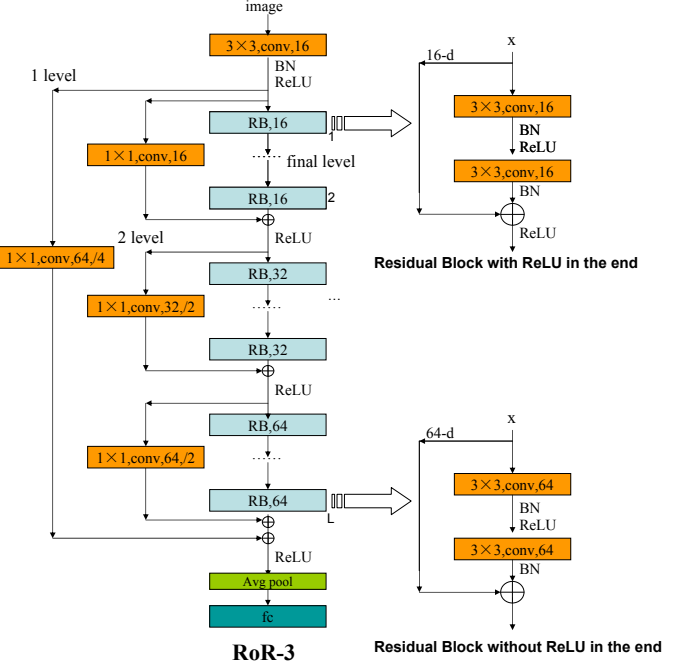


Fig. 2. RoR-3 architecture. Leftmost shortcut is root level shortcut, the rest three orange shortcuts are middle level shortcuts, the blue shortcuts are final level shortcuts. ReLU is followed by the addition. Projection shortcut is done by 1×1 convolutions. RoR adopts conv-BN-ReLU order in residual blocks.

block groups. Secondly, we add a shortcut above each residual block group, and these three shortcuts are called second level shortcuts. Then we can continue adding shortcuts as the inner level shortcuts by separating each residual block group equally. Finally, the shortcuts in original residual blocks are regarded as the final level shortcuts. Let m denote a shortcut level number, $m=1, 2, 3, \dots$. When $m=1$ RoR is an original residual networks without other shortcut level. When $m=2$, the RoR have root level and final level. In this paper, m is 3, so the RoR have root level, middle level and final level, shown in Fig. 2. Compared to the top-right residual block, the bottom-right one is without ReLU in the end, because there are extra additions following it.

When $m=3$, three residual blocks which locate the end of each residual block group can be expressed by the following formulations, and the other original residual blocks remain the same.

$$\begin{aligned} y_{L/3} &= g(x_1) + h(x_{L/3}) + F(x_{L/3}, W_{L/3}), \\ x_{L/3+1} &= f(y_{L/3}) \end{aligned} \quad (3)$$

$$\begin{aligned} y_{2L/3} &= g(x_{L/3+1}) + h(x_{2L/3}) + F(x_{2L/3}, W_{2L/3}), \\ x_{2L/3+1} &= f(y_{2L/3}) \end{aligned} \quad (4)$$

$$\begin{aligned} y_L &= g(x_1) + g(x_{2L/3+1}) + h(x_L) + F(x_L, W_L), \\ x_{L+1} &= f(y_L) \end{aligned} \quad (5)$$

Where x_l and x_{l+1} are input and output of the l -th block, and F is a residual mapping function, $h(x_l) = x_l$ and $g(x_l) = x_l$ are both identity mapping functions. $g(x_l)$ expresses the identity mapping of the first level and second level shortcuts, and $h(x_l)$ denotes the identity mapping of the final level shortcuts. $g(x_l)$ function is type B projection shortcut [12].

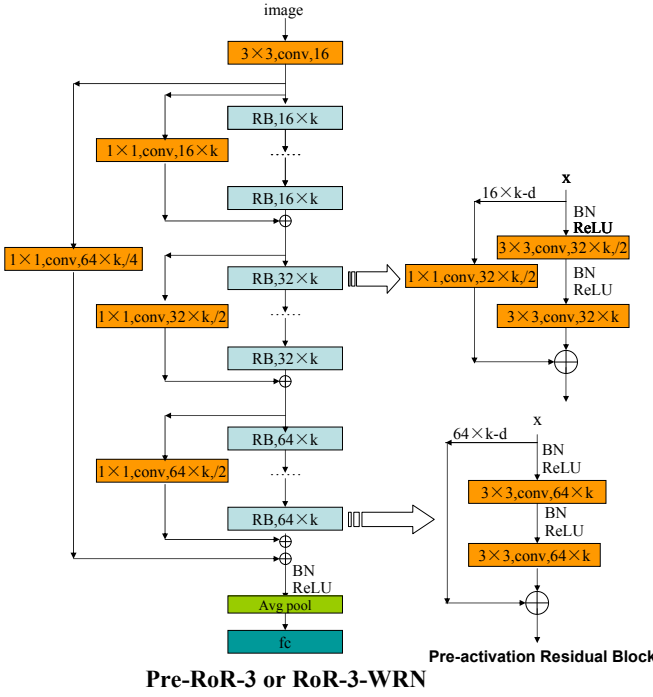


Fig. 3. Pre-RoR-3 and RoR-3-WRN architectures. $m=3$. The addition is followed by the ReLU. Projection shortcut is done by 1×1 convolutions. BN-ReLU-conv order in residual blocks is adopted. If $k=1$, this is a Pre-RoR-3 architecture, otherwise this is a RoR-3-WRN architecture. There are several direct paths for propagating information created by identity mappings.

In this paper, we will construct RoR based on ResNets, Pre-ResNets and WRN respectively. When we use original ResNets as basic residual networks, f is ReLU function, and RoR adopts conv-BN-ReLU order in residual blocks. The architecture of RoR-3 in detail is shown in Fig. 2. RoR constructed on Pre-ResNets and WRN are named after Pre-RoR and RoR-WRN. Their order of residual blocks is BN-ReLU-conv, and all $g(x_l)$, $h(x_l)$ and f functions are identity mapping. The formulations of the three different residual blocks are changed by the following formulas. The architecture of Pre-RoR and RoR-WRN in detail is shown in Fig. 3.

$$x_{L/3+1} = g(x_1) + h(x_{L/3}) + F(x_{L/3}, W_{L/3}) \quad (6)$$

$$x_{2L/3+1} = g(x_{L/3+1}) + h(x_{2L/3}) + F(x_{2L/3}, W_{2L/3}) \quad (7)$$

$$x_{L+1} = g(x_1) + g(x_{2L/3+1}) + h(x_L) + F(x_L, W_L) \quad (8)$$

IV. THE OPTIMIZATION OF ROR

In order to optimize RoR, we must determine some important parameters and principles, such as shortcut level number, identity mapping type, maximum epoch number and whether using drop-path.

A. Shortcut level number of RoR

It is important to choose suitable level number of RoR for satisfying performance. The greater shortcut level number we choose, the more branches and parameters are added. The over-fitting problem will be exacerbated, and the performance

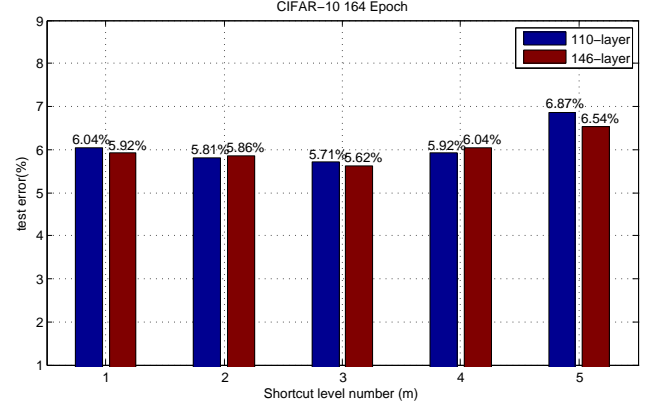


Fig. 4. Comparison of RoR with different shortcut level m . When $m=1$, it is the original ResNets. When $m=3$, RoR reaches the best performance.

may be decreasing. However, the enhancement using RoR will be less obvious once the number is too small. So we must find the suitable number to keep the balance of these two. We do some experiments on CIFAR-10 with different depth and shortcut level number, and the results are described in Fig. 4. We find out the performance of RoR ($m=3$) to be the best of all, and the performance of RoR ($m=4$ or 5) are worse than the original ResNets ($m=1$). So in this paper we choose $m=3$, which is shown in Fig. 2 and denoted as RoR-3.

B. Identity Mapping Types of RoR

He et al. [12] has investigated three types of projection shortcuts: (A) zero-padding shortcuts are used for increasing dimensions, and all shortcuts are parameter-free; (B) projection shortcuts (done by 1×1 convolutions) are used for increasing dimensions, and other shortcuts are identity; and (C) all shortcuts are projections. Type B is slightly better than type A, and type C is marginally better than B, but type C has too many extra parameters. So in this paper we use type A or B as the types of final level shortcuts.

CIFAR-10 has only 10 classes, the problem of over-fitting is not critical, and extra parameters will not obviously escalate over-fitting, so we use type B in the original residual blocks on CIFAR-10. Fig. 5 shows that we can achieve better performance using type B than type A on CIFAR-10. However, for CIFAR-100, which has 100 classes with less training examples, over-fitting is critical, so we use type A in the final level. Fig. 6 shows that we can achieve better performance using type A than type B on CIFAR-100. The original ResNets are used in all these experiments.

The shortcuts in level 1 and level 2 of RoR are all projection shortcuts. We use type B in these levels, because the input and output planes of these shortcuts are very different (especially level 1), and the zero-padding (type A) will bring more deviation. Table I shows that the final level using type A (on CIFAR-100) or type B (on CIFAR-10) while other levels using type B can achieve better performance than pure type A, no matter $m=2$ or $m=3$. In Table I, Type A and Type B indicate the shortcut type in all but final level.

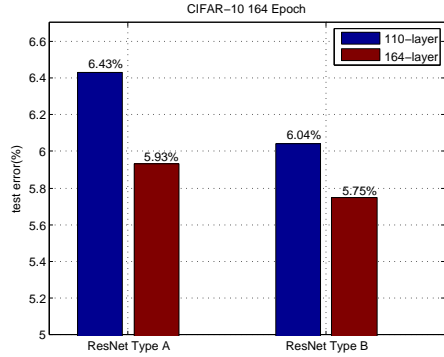


Fig. 5. Comparison of ResNets with different identity mapping types on CIFAR-10. Using type B can achieve better performance than using type A on CIFAR-10.

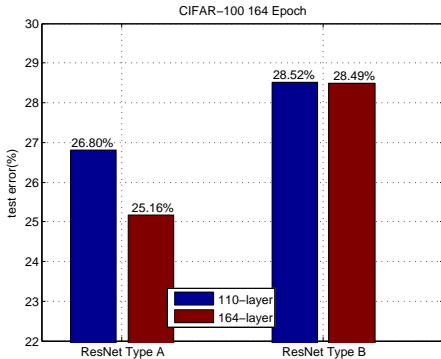


Fig. 6. Comparison of ResNets with different identity mapping types on CIFAR-100. Using type B can achieve better performance than using type A on CIFAR-10.

TABLE I
TEST ERROR (%) ON CIFAR-10/100 WITH DIFFERENT SHORTCUT TYPE
AND LEVEL

500 Epoch	ResNets	RoR-2	RoR-2 TypeA	RoR-3 TypeA	RoR-2 TypeB	RoR-3 TypeB
CIFAR-10 110-layer	5.43	6.32	6.32	7.45	5.22	5.08
CIFAR-100 164-layer	26.80	28.36	28.36	30.12	27.19	26.64

In the following Pre-RoR and RoR-WRN experiments, we find the results are comparable whether we use type B or type A in the final level on CIFAR-10. So in order to keep consistent with shortcuts types on CIFAR-100, we all use type A in the final shortcut level and type B in the other shortcut levels.

C. Maximum Epoch Number of RoR

He et al. [12], [13] adopted 164 epochs to train CIFAR-10 and CIFAR-100, but we find this epoch number inadequate to optimize ResNets, especially for RoR. Fig. 7 and Fig. 8 show that training 500 epochs can get significant promotion. So in this paper, we choose 500 as the maximum epoch number.

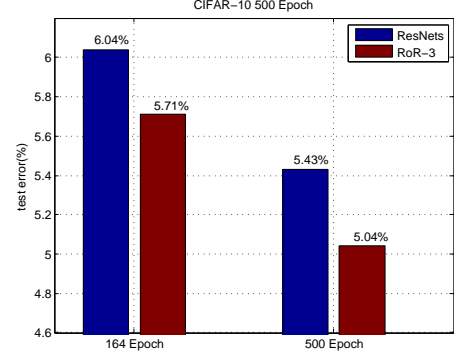


Fig. 7. Comparison of ResNets and RoR-3 with different epoch numbers on CIFAR-10. 500 epochs can achieve better performance than 164 epochs on CIFAR-10.

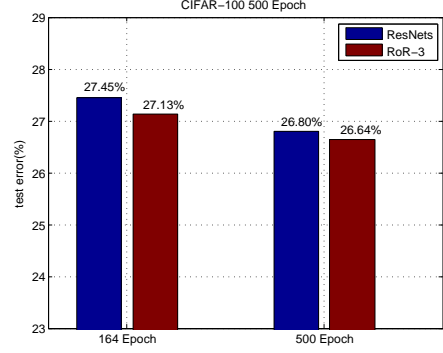


Fig. 8. Comparison of ResNets and RoR-3 with different epoch numbers on CIFAR-100. 500 epochs can achieve better performance than 164 epochs on CIFAR-100.

D. Drop Path by Stochastic Depth

Over-fitting problem is critical for CIFAR-100 dataset. When we add extra shortcuts to original ResNets, the over-fitting may be more severe. So our RoR must employ a method to alleviate over-fitting problem. The frequently used methods are dropout [35], [36] and drop-path [37], which modify interactions between sequential network layers in order to discourage co-adaptation. Dropout is less effective when used in convolutional layer, and the results of WRN [14] also proved that the effect of dropout in residual networks was unapparent. So we do not employ dropout in RoR. Drop-path prevents co-adaptation of parallel paths by randomly dropping the path. He et al. [13] has proved that the network fails to converge to a good solution by dropping identity mapping path randomly, because dropping identity mapping path greatly influences training. However, Huang et al. [15] proposed a stochastic depth drop-path method which only dropped the residual mapping path randomly. Their experiments showed that this method reduced the test errors significantly. So in this paper we use stochastic depth drop-path method in our RoR, and it can significantly alleviate over-fitting, especially on CIFAR-100 dataset.

V. EXPERIMENTS

We empirically demonstrate the effectiveness of RoR on a series of benchmark datasets: CIFAR-10, CIFAR-100, and

TABLE II
TEST ERROR (%) ON CIFAR-10 RESNETS AND ROR

CIFAR-10 500 Epoch	ResNets	ResNets+SD	RoR-3	RoR-3+SD
110-layer	5.43	5.63	5.08	5.04
164-layer	5.07	5.06	4.86	4.90

SVHN.

A. Implementation

For all datasets we compare between the results of RoR and original ResNets baseline, and other state-of-the-art methods. In the case of CIFAR, we use the same 110-layer and 164-layer ResNets used by [12] to construct RoR architecture. The original ResNets contains three groups (16 filters, 32 filters and 64 filters) of residual blocks, the feature map sizes are 32, 16 and 8 respectively. 110-layer RoR contains 18 final residual blocks, 3 middle level residual blocks (every middle level residual block contains 6 final residual blocks), and 1 root level residual block (the root level residual block contains 3 middle level residual blocks). 164-layer RoR contains 27 final residual blocks, 3 middle level residual blocks (every middle level residual block contains 9 final residual blocks), and 1 root level residual block. Our implementations are based on Torch 7 with one Nvidia Geforce Titan X. We adopt batch normalization (BN) [25] after each convolution in residual mapping paths and before activation (ReLU) [21], as shown in Fig. 2. In Pre-RoR and RoR-WRN experiments, we adopt BN-ReLU-conv order, as shown in Fig. 3. We initialize the weights as in [23]. For CIFAR datasets, we use SGD with a mini-batch size of 128 for 500 epochs. The learning rate starts from 0.1, and it is divided by a factor of 10 after epoch 250 and 375 as in [15]. For SVHN dataset, we use SGD with a mini-batch size of 128 for 50 epochs. The learning rate starts from 0.1, and it is divided by a factor of 10 after epoch 30 and 35 as in [15]. We use a weight decay of 1e-4, momentum of 0.9, and Nesterov momentum with 0 dampening on all datasets [38]. For stochastic depth drop-path method, we set p_l with the linear decay rule of $p_0 = 1$ and $p_L = 0.5$ [15].

B. CIFAR-10 Classification by RoR

CIFAR-10 is a dataset of 60,000 32×32 color images, with 10 classes of natural scene objects. The training set and test set contain 50,000 and 10,000 images. Two standard data augmentation techniques [12], [13], [14], [15] are adopted in our experiments: random sampling and horizontal flipping. We preprocess the data by subtracting the mean and dividing the standard deviation.

In Table II and Fig. 9, 110-layer ResNets without SD results in a competitive 5.43% error on the test set. 110-layer RoR-3 without SD results in a 5.08% error on the test set, and it outperforms 110-layer ResNets without SD by 6.4% on CIFAR-10 with the similar number of parameters. 164-layer RoR-3 without SD results in a 4.86% error on the test set, and it outperforms 164-layer ResNets without SD by 4.1%. As can be observed, 164-layer RoR-3 without SD can also outperform the 4.92% error of 1001-layer Pre-ResNets with

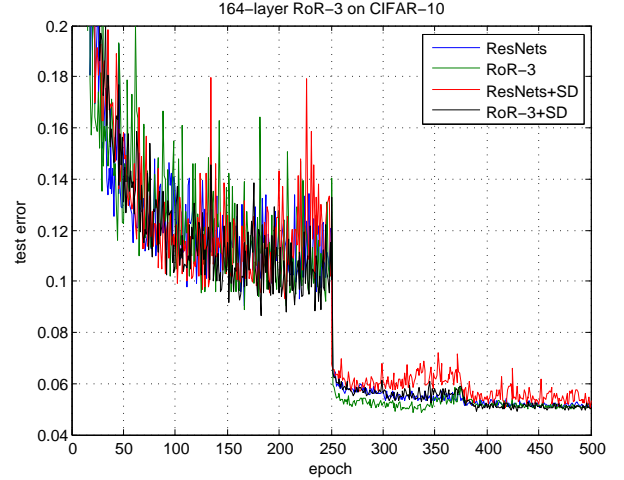


Fig. 9. Test error on CIFAR-10 by ResNets, RoR-3, ResNets+SD and RoR-3+SD during training, corresponding to results in Table II. Either RoR-3 without SD (the green curve) or RoR-3+SD (the black curve) yield lower test error than ResNets.

TABLE III
TEST ERROR (%) ON CIFAR-100 RESNETS AND ROR

CIFAR-100 500 Epoch	ResNets	ResNets+SD	RoR-2	RoR-2+SD	RoR-3	RoR-3+SD
110-layer	26.80	23.83	27.19	23.60	26.64	23.48
164-layer	25.85	23.29	-	-	27.45	22.47

the same mini-batch size [13]. We then add SD on ResNets and RoR-3 respectively, but performances are similar to the models without SD. We analyze that over-fitting on CIFAR-10 is not critical, and SD is not effective. However, adding SD can reduce training time [15] and does not affect the performance, so we add SD in the following experiments on CIFAR-10.

C. CIFAR-100 Classification by RoR

Similar to CIFAR-10, CIFAR-100 is a dataset of 60,000 32×32 color images, but with 100 classes of natural scene objects. The training set and test set contain 50,000 and 10,000 images. The augmentation and preprocessing techniques adopted in our experiments are the same as on CIFAR-10.

In Table III and Fig. 10, 110-layer and 164-layer ResNets without SD result in competitive 26.80% and 25.85% error on the test set, but the results of 110-layer RoR-3 and 164-layer RoR-3 without SD are not ideal. We argue that this is because adding extra branches and convolutional layers may escalate over-fitting. It is gratifying that 110-layer RoR-3+SD and 164-layer RoR-3+SD result in 23.48% and 22.47% error on the test set, and they outperform 110-layer ResNets, 110-layer ResNets+SD, 164-layer ResNets and 164-layer ResNets+SD by 12.4%, 1.5%, 13.1% and 3.5% respectively on CIFAR-100. We analyze that SD drop-path can alleviate over-fitting, so we will add SD in next experiments on CIFAR-100. In addition, we observe that the optimization ability of RoR-2 is better than original ResNets, but worse than RoR-3, and that is why we choose $m=3$.

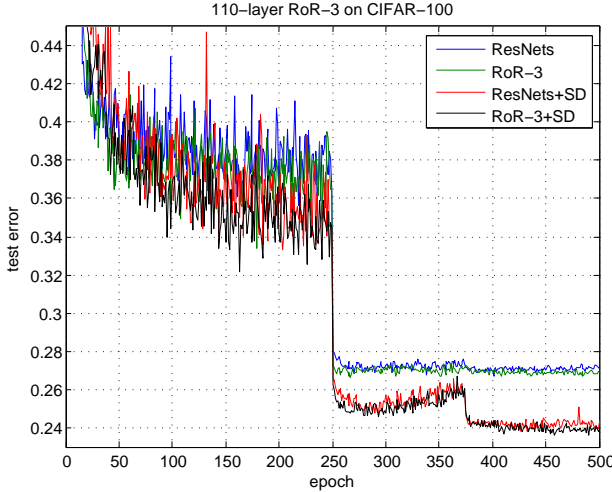


Fig. 10. Test error on CIFAR-100 by ResNets, RoR-3, ResNets+SD and RoR-3+SD during training, corresponding to results in Table III. RoR-3+SD (the black curve) yields lower test error than other curves.

TABLE IV
TEST ERROR (%) ON CIFAR-10 WITH DIFFERENT BLOCK SIZE

CIFAR-10	RoR-3 B(3,3)	RoR-3 B(3,3,3)	RoR-4 B(3,3)	RoR-4 B(3,3,3)
164-layer 164 Epoch	6.34	5.77	5.94	5.21
164-layer 500 Epoch	4.86	5.12	5.09	5.20

D. Residual Block Size Analysis

In above experiments, we use the residual block with two 3×3 convolution layers B(3,3) [12]. In order to analyze the effects of different residual block sizes, we increase the convolution layer number of every residual block to three, and the new residual block is denoted by B(3,3,3). The results are shown in Table IV. When epoch number is 164, we can achieve better performance by B(3,3,3). But if epoch number is 500 (RoR fully trained), we can find the results by B(3,3) is better than by B(3,3,3). WRN [14] try more kinds of residual blocks, and B(3,3) remain the best residual block type and size. So we choose B(3,3) as the basic residual block size in RoR. Again, we certificate the importance of 500 epochs and $m=3$.

E. Versatility of RoR for other residual networks

Recently there are several variants of residual networks which can improve the performance of original ResNets [12]. For example, Pre-ResNets [13] can reduce vanishing gradients by BN-ReLU-conv order, and WRN [14] can achieve dramatic performance increase by adding more feature planes based on Pre-ResNets. In this paper, we construct RoR architecture based on these two residual networks.

Firstly, we change the residual blocks of original RoR with BN-ReLU-conv order, and we can do the modification by only adding two levels shortcuts on the Pre-ResNets. Fig. 3 shows the architecture of Pre-RoR ($k=1$) in detail. We do the

TABLE V
TEST ERROR (%) ON CIFAR-10/100 BY PRE-RESNETS AND PRE-RoR

500 Epoch	Pre-ResNets	Pre-RoR-3	Pre-ResNest+SD	Pre-RoR-3+SD
164-layer CIFAR-10	5.04	5.02	4.67	4.51
164-layer CIFAR-100	25.54	25.33	22.49	21.94

TABLE VI
TEST ERROR (%) ON CIFAR-10/100 BY WRN AND RoR-WRN

500 Epoch	WRN40-2	RoR-3-WRN40-2	WRN40-2+SD	RoR-3-WRN40-2+SD
CIFAR-10	4.81	5.01	4.80	4.59
CIFAR-100	24.70	25.19	22.87	22.48

same experiment by Pre-RoR-3 on CIFAR-10 and CIFAR-100, and show the results in Table V where we compare Pre-RoR with Pre-ResNets. As can be observed, 164-layer Pre-RoR-3+SD achieves the surprising 4.51% error on CIFAR-10 and 21.94% error on CIFAR-100. Particularly, 164-layer Pre-RoR-3+SD can outperform 164-layer Pre-ResNets and 164-layer Pre-ResNets+SD by 14.1% and 2.4% on CIFAR-100.

Secondly, we use $(16 \times k, 32 \times k, 64 \times k)$ filters instead of $(16, 32, 64)$ filters of original Pre-RoR, as WRN is constructed based on Pre-ResNets. Fig. 3 shows the architecture of RoR-WRN ($k=2, 4$) in detail. We do the same experiment by RoR-3-WRN on CIFAR-10 and CIFAR-100, and show the results in Table VI. Fig. 11 and Fig. 12 show the test errors on CIFAR-10 and CIFAR-100 at different training epochs. As can be observed, the performance of RoR-3-WRN is worse than WRN. In our opinion, WRN has more feature planes, so it is easier to get over-fitting when we add extra branches and parameters. SD can alleviate over-fitting, so the performance of RoR-3-WRN+SD is better than others. RoR-3-WRN40-2+SD achieves 4.59% error on CIFAR-10 and 22.48% error on CIFAR-100.

Through analysis and experiments, we can prove that our RoR architecture can also promote optimization abilities of other residual networks, such as Pre-ResNets and WRN. Because RoR has good versatility for other residual networks, we have reasons to believe that our RoR has a good application prospect in residual networks family.

F. Depth and Width Analysis

According to above experiments, we find that the performance can be improved by increasing depth or width. In this section we analyze how to choose depth and width of RoR.

The basic RoR is based on original ResNets, but very deep ResNets encounter serious vanishing gradients problem. So even though the performance of RoR is better than ResNets, RoR still can not resolve vanishing problem. We repeat the RoR experiments by increasing number of convolutional layers, and show the results in Table VII. As can be observed, when number of layers increase from 164 to 182, then to 218, the performance gradually decreases. These experiments

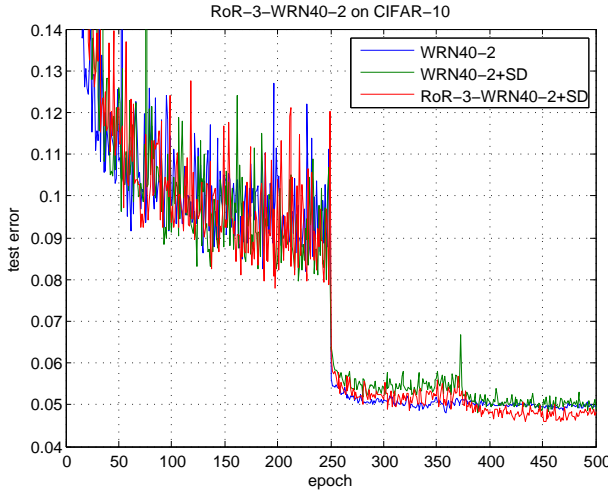


Fig. 11. Test error on CIFAR-10 by WRN40-2, WRN40-2+SD and RoR-3-WRN40-2+SD during training, corresponding to results in Table VI. RoR-3-WRN40-2+SD (the red curve) yield lower test error than other curves.

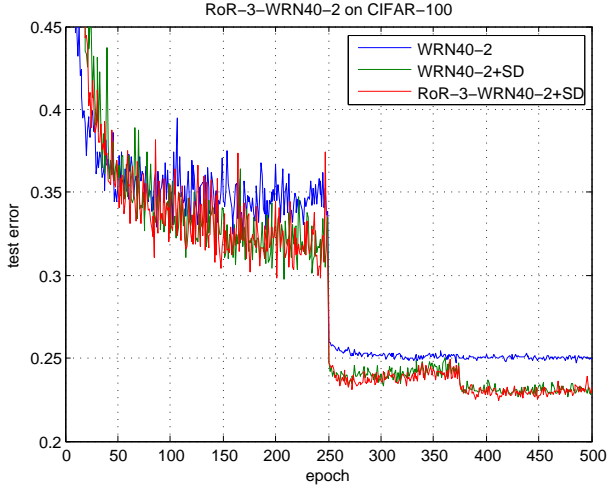


Fig. 12. Test error on CIFAR-100 by WRN40-2, WRN40-2+SD and RoR-3-WRN40-2+SD during training, corresponding to results in Table VI. RoR-3-WRN40-2+SD (the red curve) yield lower test error than other curves.

TABLE VII
TEST ERROR (%) ON CIFAR-10/100 BY ROR WITH DIFFERENT DEPTH

Depth	CIFAR-10 Ror-3 without SD	CIFAR-100 Ror-3+SD
110-layer	5.08	23.48
164-layer	4.86	22.47
182-layer	4.98	22.76
218-layer	5.12	22.99

demonstrate that the vanishing problem exists in very deep RoR.

Pre-ResNets can reduce vanishing problem, so Pre-RoR should inherit this property too. We repeat the Pre-RoR experiments by increasing number of convolutional layers, and the results are shown in Table VIII. We observe that the accuracy increases as the number of layer increases. 1202-layer Pre-

TABLE VIII
TEST ERROR (%) ON CIFAR-10/100 BY PRE-ROR WITH DIFFERENT DEPTH

Depth	CIFAR-10 Pre-RoR-3+SD	CIFAR-100 Pre-RoR-3+SD
110-layer	4.63	23.05
164-layer	4.51	21.94
218-layer	4.51	21.43
1202-layer with 32 mini-batch size	4.49	20.64

TABLE IX
TEST ERROR (%) ON CIFAR-10/100 BY ROR-WRN WITH DIFFERENT DEPTH AND WIDTH

Depth and Width	CIFAR-10 Ror-3-WRN+SD	CIFAR-100 Ror-3-WRN+SD
RoR-3-WRN40-2	4.59	22.48
RoR-3-WRN40-4	4.09	22.11
RoR-3-WRN58-2	4.23	21.50
RoR-3-WRN58-4	3.77	19.73

RoR-3+SD with a mini-batch size of 32 achieve the 4.49% error on CIFAR-10 and 20.64% error on CIFAR-100. These results mean that the vanishing gradients can be reduced, even on very deep models. So we can use Pre-RoR to push the limit of depth.

WRN is not very deep, so the vanishing problem is not obvious. However, over-fitting maybe becomes severe because of adding more feature planes and parameters. We do the same experiments by RoR-WRN with different depth and width on CIFAR-10 and CIFAR-100, and show the results in Table IX. We find both deepening and widening the network can improve the performance. But when we widen the RoR-WRN, weight parameters increase exponentially. So we must complement RoR-WRN by SD to reduce over-fitting. As can be observed, RoR-3-WRN-58-4+SD achieves the extraordinary 3.77% error on CIFAR-10 and 19.73% error on CIFAR-100. We find that the RoR-WRN with the similar order of magnitude parameters is more effective than Pre-RoR, because the vanishing problem already exists in very deep Pre-RoR.

Through experiments and analysis, we elucidate that the depth and width of RoR are equally important to model learning capability. We must carefully choose suitable depth and width on the given task to achieve satisfying results. In this paper we propose a two-step strategy to choose depth and width. We should first increase the depth of RoR gradually until the performance is saturated. Then increase the width of RoR gradually until we achieve the best results.

G. SVHN Classification by RoR

The Street View House Number (SVHN) dataset that we use contains 32×32 colored images of cropped out house numbers from Google Street View. The task is to classify the digit at

TABLE X
TEST ERROR (%) ON SVHN BY WRN58-4, WRN58-4+SD,
WRN58-4+SD AND ROR-3-WRN58-4+SD

50 Epoch	WRN58-4	RoR-3-WRN58-4	WRN58-4+SD	RoR-3-WRN58-4+SD
SVHN	1.69	1.66	1.66	1.59

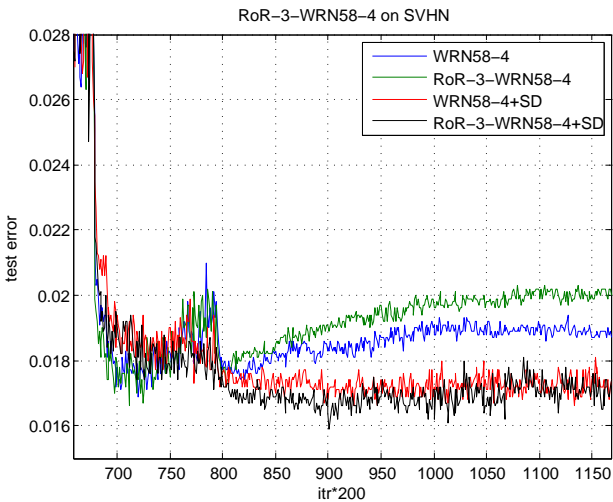


Fig. 13. Test error on SVHN by WRN58-4RoR-3-WRN58-4, WRN58-4+SD and RoR-3-WRN58-4+SD during training. RoR-3-WRN58-4+SD (the black curve) yield lower test error than the curves.

center (and ignore any additional digit that might appear on the side) of images. There are 73,257 digits in the training set, 26,032 in the test set and 531,131 easier samples for additional training. Following the common practice, we use all the training samples but do not perform data augmentation. We preprocess the data by subtracting the mean and dividing the standard deviation. Batch size is set to 128, and test error is calculated every 200 iterations. We use our best architecture RoR-3-WRN58-4+SD to train SVHN and achieve the excellent result 1.59% test error, as shown in Table X. This result outperforms WRN58-4 and WRN58-4+SD by 5.9% and 4.2% on SVHN respectively, and Fig. 13 shows the test error at different training epochs. We can see that the results of WRN58-4 and RoR-3-WRN58-4 are good as well, but they start to overfit after 700×200 iterations.

H. Comparisons with state-of-the-art results on CIFAR-10/100 and SVHN

Table XI compares with the state-of-the-art methods on CIFAR-10/100 and SVHN, where we achieve overwhelming results. We obtain these results via a simple concept — the residual mapping of residual mapping should be easier to optimize. We remark that we do not use complicated architectures and any other tricks, adding only two shortcut levels with thousands of parameters makes original residual networks better optimized. For data augmentation, RoR uses no more than naive translation and horizontal flipping, while other methods may adopt more complicated data augmentation techniques. Our 164-layer RoR-3 has an error of 4.86% on CIFAR-10,

TABLE XI
TEST ERROR (%) ON CIFAR-10, CIFAR-100 AND SVHN BY DIFFERENT METHODS

Method(#Parameters)	CIFAR-10	CIFAR-100	SVHN
NIN [5]	8.81	35.68	2.35
FitNet [8]	8.39	35.04	2.42
DSN [9]	7.97	34.57	1.92
All-CNN [10]	7.25	33.71	-
Highway [28]	7.72	32.39	-
ELU [22]	6.55	24.28	-
FractalNet (30M) [29]	4.59	22.85	1.87
ResNets-164 (2.5M) [12] (reported by [13])	5.93	25.16	-
FitResNet, LSUV [26]	5.84	27.66	-
Pre-ResNets-164 (2.5M) [13]	5.46	24.33	-
Pre-ResNets-1001 (10.2M) [13]	4.62	22.71	-
ELU-ResNets-110 (1.7M) [31]	5.62	26.55	-
PELU-ResNets-110 (1.7M) [24]	5.37	25.04	-
ResNets-110+SD (1.7M) [15]	5.23	24.58	1.75 (152-layer)
ResNet in ResNet (10.3M) [30]	5.01	22.90	-
SwapOut (7.4M) [32]	4.76	22.72	-
WResNet-d (19.3M) [33]	4.70	-	-
WRN28-10 (36.5M) [14]	4.17	20.50	1.64
CRMN-28 (more than 40M) [34]	4.65	20.35	1.68
RoR-3-164 (2.5M)	4.86	22.47	-
Pre-RoR-3-164 (2.5M)	4.51	21.94	-
RoR-3-WRN40-2 (2.2M)	4.59	22.48	-
Pre-RoR-3-1202 (19.4M)	4.49	20.64	-
RoR-3-WRN40-4 (8.9M)	4.09	20.11	-
RoR-3-WRN58-4 (13.3M)	3.77	19.73	1.59

which is better than 4.92% of 1001-layer Pre-ResNets with the same batch size. Our 164-layer RoR-3+SD has an error of 22.47% on CIFAR-100, which is better than 22.71% of 1001-layer Pre-ResNets. Most importantly, it is not only suitable to the original ResNets but also other kinds of residual networks (Pre-ResNets and WRN). The performance of our Pre-RoR-3 and RoR-3-WRN outperform original Pre-ResNets and WRN. Particularly, our RoR-3-WRN58-4+SD gets single-model error of 3.77% on CIFAR-10, 19.73% on CIFAR-100 and 1.59% on SVHN, which are the new state-of-the-art performances to our knowledge. These results demonstrate the effectiveness and versatility of RoR. No matter what kinds of basic residual networks, RoR can always achieve better results than its basic residual networks with same number of layers.

Although some variants of residual networks (WRN and CRMN) or other CNNs (FractalNet) can achieve competitive results, the number of parameters in these models is too large (shown in Table XI). Through experiments and analysis, we argue that our RoR method can outperform other methods with similar order of magnitude parameters. Our RoR models with about only 3M parameters (Pre-RoR-3-164, RoR-3-WRN40-2

and Pre-RoR-3-218) can outperform FractalNet (30M parameters) and CRMN-28 (more than 40M parameters) on CIFAR-10. Our RoR-3-WRN40-4 model with 8.9M parameters can outperform all of the exiting methods. Our best RoR-3-WRN58-4 model with 13.3M parameters achieves the new state-of-the-art performance. We have reasons to argue that better performance can be achieved by additional depth and width.

VI. CONCLUSION

This paper proposes a new Residual networks of Residual networks architecture (RoR), which obtains new state-of-the-art performance on CIFAR-10, CIFAR-100 and SVHN for image classification. Through empirical studies, this work not only significantly advances the image classification performance, but also provides an effective complement of residual networks family in the future. In other words, whatever residual network it is, it can be improved by RoR. That is to say, RoR has a good prospect of application on various image recognition tasks.

ACKNOWLEDGMENT

The authors would like to thank the editor and the anonymous reviewers for their careful reading and valuable remarks.

REFERENCES

- [1] Y. LeCun, Y. Bengio, and G. Hinton, “Deep learning,” *Nature*, vol. 521, no. 7553, pp. 436–444, May. 2015.
- [2] A. Krizhevsky, I. Sutskever, and G. Hinton, “Imagenet classification with deep convolutional networks,” in *Proc. Adv. Neural Inf. Process. Syst.*, 2012, pp. 1097–1105.
- [3] W. Y. Zou, X. Y. Wang, M. Sun, and Y. Lin, “Generic object detection with dense neural patterns and regional,” *arXiv preprint arXiv:1404.4316*, 2014.
- [4] J. Deng, W. Dong, R. Socher, L. J. Li, K. Li, and L. Fei-Fei, “Imagenet: A large-scale hierarchical image database,” in *Proc. IEEE Conf. Comput. Vis. Pattern Recog.*, 2009, pp. 248–255.
- [5] M. Lin, Q. Chen, and S. Yan, “Network in network,” *arXiv preprint arXiv:1312.4400*, 2013.
- [6] P. Sermanet, D. Eigen, X. Zhang, M. Mathieu, R. Fergus, and Y. LeCun, “Overfeat: Integrated recognition, localization and detection using convolutional networks,” *arXiv preprint arXiv:1312.6229*, 2013.
- [7] K. Simonyan, and A. Zisserman, “Very deep convolutional networks for large-scale image recognition,” *arXiv preprint arXiv:1409.1556*, 2014.
- [8] A. Romero, N. Ballas, S. E. Kahou, A. Chassang, C. Gatta, and Y. Bengio, “Fitnets: hints for thin deep nets,” *arXiv preprint arXiv:1412.6550*, 2014.
- [9] C. -Y. Lee, S. Xie, P. Gallagher, Z. Zhang, and Z. Tu, “Deeply-supervised nets,” in *Proc. AISTATS*, 2015, pp. 562–570.
- [10] J. T. Springenberg, A. Dosovitskiy, T. Brox, and M. Riedmiller, “Striving for simplicity: The all convolutional net,” *arXiv preprint arXiv:1412.6806*, 2014.
- [11] C. Szegedy, W. Liu, Y. Jia, P. Sermanet, S. Reed, D. Anguelov, D. Erhan, V. Vanhoucke, and A. Rabinovich, “Going deeper with convolutions,” in *Proc. IEEE Conf. Comput. Vis. Pattern Recog.*, 2015, pp. 1–9.
- [12] K. He, X. Zhang, S. Ren, and J. Sun, “Deep residual learning for image recognition,” *arXiv preprint arXiv:1512.03385*, 2015.
- [13] K. He, X. Zhang, S. Ren, and J. Sun, “Identity mapping in deep residual networks,” *arXiv preprint arXiv:1603.05027*, 2016.
- [14] S. Zagoruyko, and N. Komodakis, “Wide residual networks,” *arXiv preprint arXiv:1605.07146*, 2016.
- [15] G. Huang, Y. Sun, Z. Liu, and K. Weinberger, “Deep networks with stochastic depth,” *arXiv preprint arXiv:1605.09382*, 2016.
- [16] A. Krizhevsky, and G. Hinton, “Learning multiple layers of features from tiny images,” M.Sc. thesis, Dept. of Comput. Sci., Univ. of Toronto, Toronto, ON, Canada, 2009.
- [17] Y. Netzer, T. Wang, A. Coates, A. Bissacco, B. Wu, and A. Y. Ng, “Reading digits in natural images with unsupervised feature learning,” in *Proc. NIPS Workshop Deep Learning and Unsupervised feature learning.*, 2011, pp. 1–9.
- [18] Y. Bengio, P. Simard, and P. Frasconi, “Learning long-term dependencies with gradient descent is difficult,” *IEEE Trans. Neural Networks*, vol. 5, no. 2, pp. 157–166, Aug. 2014.
- [19] X. Glorot, and Y. Bengio, “Understanding the difficulty of training deep feedforward neural networks,” in *Proc. Conf. Art. Intell. Stat.*, 2010, pp. 249–256.
- [20] D. Erhan, Y. Bengio, A. Courville, P. A. Manzagol, P. Vincent, and S. Bengio, “Why does unsupervised pre-training help deep learning?,” *The Journal of Machine Learning Research*, vol. 11, pp. 625–660, Mar. 2010.
- [21] V. Nair, and G. Hinton, “Rectified linear units improve restricted Boltzmann machines,” in *Proc. ICML*, 2010, pp. 807–814.
- [22] D. -A. Clevert, T. Unterthiner, and S. Hochreiter, “Fast and accurate deep network learning by exponential linear units (elus),” *arXiv preprint arXiv:1511.07289*, 2015.
- [23] K. He, X. Zhang, S. Ren, and J. Sun, “Delving deep into rectifiers: Surpassing human-level performance on imagenet classification,” *arXiv preprint arXiv:1502.01852*, 2015.
- [24] L. Trottier, P. Giguere, and B. Chaib-draa, “Parametric exponential linear unit for deep convolutional neural networks,” *arXiv preprint arXiv:1605.09322*, 2016.
- [25] S. Ioffe, and C. Szegedy, “Batch normalization: accelerating deep network training by reducing internal covariate shift,” *arXiv preprint arXiv:1502.03167*, 2015.
- [26] D. Mishkin, and J. Matas, “All you need is a good init,” *arXiv preprint arXiv:1511.06422*, 2015.
- [27] K. He, and J. Sun, “Convolutional neural networks at constrained time cost,” in *Proc. IEEE Conf. Comput. Vis. Pattern Recog.*, 2015, pp. 5353–5360.
- [28] R. K. Srivastava, K. Greff, and J. Schmidhuber, “Highway networks,” *arXiv preprint arXiv:1505.00387*, 2015.
- [29] G. Larsson, M. Maire, and G. Shakhnarovich, “FractalNet: ultra-deep neural networks without residuals,” *arXiv preprint arXiv:1605.07648*, 2016.
- [30] S. Targ, D. Almeida, and K. Lyman, “Resnet in resnet: generalizing residual architectures,” *arXiv preprint arXiv:1603.08029*, 2016.
- [31] A. Shah, S. Shinde, E. Kadam, and H. Shah, “Deep residual networks with exponential linear unit,” *arXiv preprint arXiv:1604.04112*, 2016.
- [32] S. Singh, D. Hoiem, and D. Forsyth, “Swapout: learning an ensemble of deep architectures,” *arXiv preprint arXiv:1605.06465*, 2016.
- [33] F. Shen, and G. Zeng, “Weighted residuals for very deep networks,” *arXiv preprint arXiv:1605.08831*, 2016.
- [34] J. Moniz, and C. Pal, “Convolutional residual memory networks,” *arXiv preprint arXiv:1606.05262*, 2016.
- [35] G. Hinton, N. Srivastava, A. Krizhevsky, and K. Weinberger, “Improving neural networks by preventing co-adaptation of feature detectors,” *arXiv preprint arXiv:1207.0580*, 2012.
- [36] N. Srivastava, G. Hinton, A. Krizhevsky, I. Sutskever, and R. Salakhutdinov, “Dropout: a simple way to prevent neural networks from overfitting,” *The Journal of Machine Learning Research*, vol. 15, pp. 1929–1958, Jun. 2014.
- [37] L. Wan, M. Zeiler, S. Zhang, Y. L. Cun, and R. Fergus, “Regularization of neural networks using dropconnect,” in *Proc. ICML*, 2013, pp. 1058–1066.
- [38] S. Gross, and M. Wilber, ” Training and investigating residual nets,” Facebook AI Research, CA. [Online]. Available:<http://torch.ch/blog/2016/02/04/resnets.html>, 2016.